Kinetics of the Decay Reactions of the *N*,*N*-Dimethyl-*p*-Toluidine Cation Radical in Acetonitrile. Acid−Base Interaction to Promote the CH_2-CH_2 Bonding

Masashi Goto, Hyun Park,† and Koji Otsuka

Department of Material Chemistry, Graduate School of Engineering, Kyoto University, Sakyo-ku, Kyoto 606-8501, Japan

Munetaka Oyama*

Division of Research Initiatives, International Innovation Center, Kyoto University, Sakyo-ku, Kyoto 606-8501, Japan

Received: May 7, 2002; In Final Form: June 26, 2002

The decay reaction of *N*,*N*-dimethyl-*p*-toluidine (DMT) cation radical (DMT•$^+$) in acetonitrile (AN) was analyzed using an electron-transfer stopped-flow (ETSF) method. In the ETSF method, DMT•$^+$ is generated by mixing AN solutions of DMT and tris(*p*-bromophenyl)amine cation radical (TBPA•$^+$). When DMT•$^+$ was generated quantitatively without DMT via 1:1 mixing of DMT and TBPA•$^+$, it was found that DMT•$^+$ was fairly stable in AN. On the other hand, when DMT remained with DMT•$^+$ under the control of the mixing ratio of DMT/TBPA•$^+$ (> 1), the neutral DMT was found to promote the decay reaction of DMT•$^+$. From the determined rate law, $-d[DMT\bullet^+]/dt = k\,[DMT\bullet^+]\,[DMT]$ ($k = 6.5 \times 10^2$ M^{-1} s^{-1}), the initial acid−base reaction between DMT•$^+$ and DMT was clarified to be the rate determining step. The acid−base interaction was also confirmed by observing the decay reaction of DMT•$^+$ in the presence of pyridine derivatives. The identical rate law, which indicates the rate-determining acid−base interaction, was obtained for eight pyridine derivatives examined, though the final product was different from the case of DMT. The ETSF method has permitted the straightforward analysis and given a definite kinetic conclusion concerning the acid−base reaction between DMT•$^+$ and DMT.

Introduction

Numerous studies have been devoted to the kinetic analysis of aromatic cation radicals in aprotic solvents,[1] and work still continues in this area.[2−9] In addition to cation radical−nucleophile combination reactions, proton-transfer reactions have been analyzed because of the acidic property of cation radicals to release H^+.[2] By analyzing the reaction of cation radicals with bases, such as pyridine derivatives, the recent advances have shown the detailed mechanism of the proton-transfer reactions.[4,5]

When we consider the acidic property of aromatic cation radicals, it may be necessary to elucidate the property as a base of the neutral molecules, in particular, in the cases of aromatic amine cation radicals as discussed previously.[8,9] In a previous communication,[10] we have analyzed the reaction of the *N*,*N*-dimethyl-*p*-toluidine (DMT, Figure 1) cation radical (DMT•$^+$) in acetonitrile (AN) using an electron-transfer stopped-flow (ETSF) method, in which DMT•$^+$ was generated via the electron-transfer reaction between DMT and tris(*p*-bromophenyl)amine (TBPA) cation radical (TBPA•$^+$). In the ETSF method, the amount of neutral molecules coexisting with the cation radicals can be easily controlled.[10−15] Utilizing this technique, the effect of DMT on the decay reaction of DMT•$^+$ was analyzed to form *N*,*N*,*N*′,*N*′-tetramethyl-α,α′-bi-*p*-toluidine (TMBT, Figure 1),[10] while the electrochemical results on the oxidation of DMT in AN to form TMBT had been reported previously.[16,17]

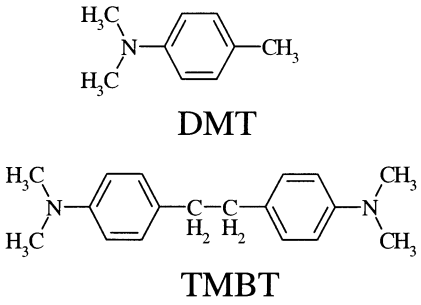

Figure 1. Structural formulas of *N*,*N*-dimethyl-*p*-toluidine (DMT) and *N*,*N*,*N*′,*N*′-tetramethyl-α,α′-bi-*p*-toluidine (TMBT).

In the present full paper, at first, the details of the reaction of DMT•$^+$ controlled by the neutral DMT are described with the ETSF analysis. In the electrochemical methods, it had been very difficult to analyze the effects of the neutral molecules explicitly because the neutral molecules surely coexist when the cation radicals are generated on the electrodes. Compared with the electrochemical results, a definite conclusion on the reaction kinetics between DMT•$^+$ and DMT is given by the results obtained using the ETSF method.

Next, the reactions of DMT•$^+$ in the presence of pyridine derivatives (X-Py s), instead of the neutral DMT, are analyzed. By mixing the solution of 0.10 mM TBPA•$^+$ with the solution containing both 0.10 mM DMT and *x* mM X-Py, the reaction between 0.050 mM DMT•$^+$ and *x*/2 mM X-Py can be observed in the absence of DMT in the ETSF method. The reaction rates

* Corresponding author. Tel: +81-75-753-9152, Fax: +81-75-753-9145, E-mail: oyama@iic.kyoto-u.ac.jp.
† Present address: POSCO, Republic of Korea.

10.1021/jp026073h CCC: $22.00
Published on Web 08/06/2002

should reflect the basic property of X-Py s as in the previous work on hexamethylbenzene cation radicals.[18] In the present work, the relationship between the basic property and the reaction rates of DMT•$^+$ is compared by determining the decay rates of DMT•$^+$ in the presence of eight X-Py s; i.e., pyridine (Py), 2-methylpyridine (2Me-Py), 4-methylpyridine (4Me-Py), 2,4-dimethylpyridine (2,4Me-Py), 2,6-dimethylpyridine (2,6Me-Py), 2,4,6-trimethylpyridine (2,4,6Me-Py), 4-cyanopyridine (4CN−Py), and 4-methoxypyridine (4MeO−Py).

In addition, the basic property of *N*,*N*-dimethylformamide (DMF) is evaluated by observing the decay reaction of DMT•$^+$ in the presence of DMF in AN. While DMF has been used as the solvent in the recent studies with the fast scan cyclic voltammetric analysis,[8,9] the basic properties of DMF and DMT are compared through the decay reaction of DMT•$^+$ in the present work.

Experimental Section

The concept and actual measurements of the ETSF method were described previously.[11,12] In this method, unstable cation radicals (N•$^+$) are formed via the electron transfer with another long-lived cation radical (M•$^+$) whose formal potential is positive to that of N•$^+$, as expressed by eq 1.

$$\mathrm{N} + \mathrm{M}\bullet^+ \rightarrow \mathrm{N}\bullet^+ + \mathrm{M} \qquad (1)$$

In the present work, DMT•$^+$ is produced via the electron-transfer reaction of eq 2.

$$\mathrm{DMT} + \mathrm{TBPA}\bullet^+ \rightarrow \mathrm{DMT}\bullet^+ + \mathrm{TBPA} \qquad (2)$$

All the measurements were carried out in AN as a solvent. Because TBPA•$^+$ is stable enough,[19] the AN solution was prepared by a batchwise electrolysis and used after diluting it to an appropriate concentration by AN. The concentration was determined by the absorption measurement using the reported molar absorptivity of TBPA•$^+$ at 705 nm, $\epsilon = 3.2 \times 10^4$ M^{-1} cm^{-1}.[19]

For the stopped-flow measurements, a rapid-scan stopped-flow spectroscopic system, RSP-601 (Unisoku Co. Ltd., Hirakata, Japan) was used. In this apparatus, dynamic transformation of absorption spectra can be observed with the minimized time interval of 1.0 ms after mixing two solutions. The obtained decay curve at a wavelength was composed of 512 points. The simulation analysis was carried out using Microsoft Excel 2000.

Cyclic voltammograms were obtained using a computer-controlled PAR 263 potentiostat. The working electrode used was a 1.6 mm diameter platinum disk electrode (BAS Co. Ltd), and the reference electrode used was a Pt | (I_3^-, I^-) electrode in AN.

Product analysis was carried out for the solution obtained after mixing the solutions of TBPA•$^+$ and 5-fold excess of DMT in the case of the reaction between DMT•$^+$ and DMT. It was evaporated to ca. 1/10 amount and extracted with ether after adding water. The extract was evaporated and separated using a silica gel column with hexane + ethyl acetate as an eluent. The isolated product was identified using a ^{1}H NMR. For the case of the reaction between DMT•$^+$ and X-Py, the products were analyzed using the same procedure after mixing the solution of TBPA•$^+$ with the solution containing both DMT and pyridine. After obtaining the authentic products identified using the ^{1}H NMR, the products in the reactions with X-Py s were confirmed by a thin-layer chromatography.

The reagents, DMT, TBPA, and X-Py s, were obtained from Aldrich, and used as received. For a solvent, acetonitrile dehydrated (Wako chemicals, H_2O < 50 ppm) was used as received. As the supporting electrolytes for the electrochemical measurement, tetrabutylammonium hexafluorophosphate (Fluka, puriss. electrochemical grade > 99.0%) was used.

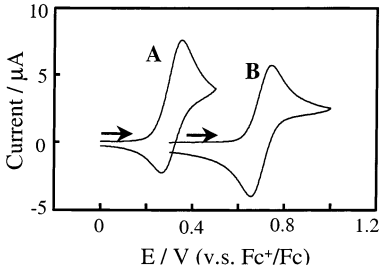

Figure 2. Cyclic voltammograms of (A) DMT and (B) TBPA in AN. Concentration of the substrates: 1.0 mM. Supporting electrolyte: tetrabutylammonium hexafluorophosphate 0.10 M. Working electrode: platinum disk electrode (diameter: 1.6 mm). Scan rate: 100 mV s^{-1}.

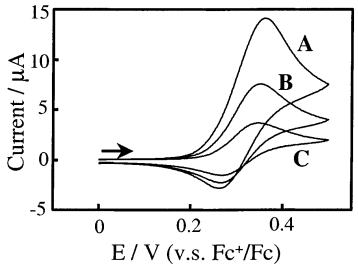

Figure 3. Cyclic voltammograms of DMT in AN. [DMT]: (A) 2.0 mM, (B) 1.0 mM, and (C) 0.50 mM. Supporting electrolyte: tetrabutylammonium hexafluorophosphate 0.10 M. Working electrode: platinum disk electrode (diameter: 1.6 mm). Scan rate: 100 mV s^{-1}.

Results and Discussion

Cyclic Voltammograms of DMT. Figure 2 shows the cyclic voltammograms of TBPA and DMT in AN. While the redox potential of TBPA•$^+$/TBPA is 0.69 V, the oxidation peak potential of DMT is 0.32 V. Because the oxidation potential of TBPA is 0.4 V positive to that of DMT, eq 2 should proceed quantitatively when the solutions of TBPA•$^+$ and DMT are mixed. In addition, some irreversibility can be recognized for the oxidation process of DMT (Figure 2A). This implies the presence of the consecutive chemical reactions of DMT•$^+$ as reported previously.[16,17]

Figure 3 shows the changes in cyclic voltammograms depending on the concentration of DMT. With increasing the concentration of DMT, the ratio of the oxidation current versus the reduction current was increased as shown in this figure, implying the presence of consecutive chemical reactions. As well as the DMT concentration, the scan rate is a factor to influence the irreversibility. When the scan rate was relatively slower, the irreversibility was increased. Actually, almost reversible response was obtained for the low concentration, 0.20 mM, DMT at the higher scan rate of 500 mV s^{-1} (data is not shown here).

Decay Reaction of DMT•$^+$ Influenced by the Presence of DMT. Generally, in electrochemical oxidation processes, the neutral molecules are necessarily present in the vicinity of the electrode to be oxidized. Thus, the complex reactions between the cation radicals and the neutral molecules might bring about some difficulties in analyzing the electrochemical responses, though the cation radical−substrate coupling is one of the typical oxidative dimerization reactions.[20] For the clear-cut observation of the reaction processes involving cation radicals and the neutral

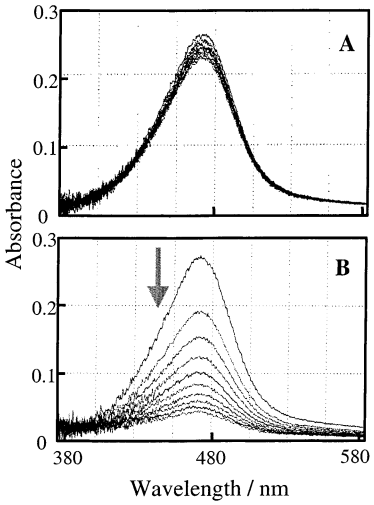

Figure 4. Changes in absorption spectra observed after mixing of the AN solution of 0.10 mM TBPA•+ with the AN solution of DMT. [DMT]: (A) 0.10 mM and (B) 1.0 mM. Time interval of each spectrum: 1.0 s. Composed of 10 spectra. While DMT•+ is almost stable without DMT as in A, monotonic decrease of DMT•+ was observed in the reaction of 0.05 mM DMT•+ with 0.45 mM DMT as shown in B.

molecules, we are proposing the ETSF method,[10−15] in which kinetic observations can be carried out in complete homogeneous solution.

Figure 4 shows the remarkable features of the reactions of DMT•+ revealed explicitly using the ETSF method. In this method, when the solutions of 0.10 mM TBPA•+ and 0.10 mM DMT were mixed, the solution of 0.05 mM DMT•+ is formed in the optical cell in the stopped-flow apparatus, considering the dilution due to the equivolume mixing. That is, the solution containing only DMT•+ without DMT can be produced easily in homogeneous solution using the ETSF method, while DMT is necessarily present in the conventional electrochemical generation of DMT•+. The absorption spectra of Figure 4A that can be reasonably assigned to that of DMT•+ judging from the complete disappearance of TBPA•+ after the mixing indicate that the decrease of DMT•+ was very little during 10 s. While the stability of the cation radicals in AN is susceptible to water content in many cases, DMT•+ was stable enough, even in the presence of H_2O. The absorption spectra of DMT•+ unaltered by 50 mM H_2O were observed using the ETSF method. In contrast, as shown in Figure 4B, the remarkable decrease of DMT•+ was observed in the reaction of 0.05 mM DMT•+ with 0.45 mM DMT, recorded after mixing the solutions of 0.10 mM TBPA•+ with 1.0 mM DMT. Figure 4B indicates clearly that the neutral DMT promotes the decay reaction of DMT•+.

Thus, two conclusions are summarized here from the results of Figure 4. First, when DMT•+ is formed quantitatively without DMT, DMT•+ is fairly stable (Figure 4A), though this situation is very difficult to prepare in electrochemical measurements. While the phenyl C−C coupling proceeds at the para position through the cation radical−cation radical coupling in the reactions of methyldiphenylamine and diphenylamine cation radicals,[11,12] the sufficient blocking effects of the *p*-methyl substituent of DMT•+ are verified to prevent the phenyl C−C coupling judging from the stability of 10 s. Second, as apparently from Figure 4B, the neutral DMT promotes the decrease of DMT•+. That is, the stability of DMT•+ is very susceptible to the neutral DMT.

Kinetic Analysis of the Reaction between DMT•+ and DMT. To make clear the effects of DMT on the decay reaction

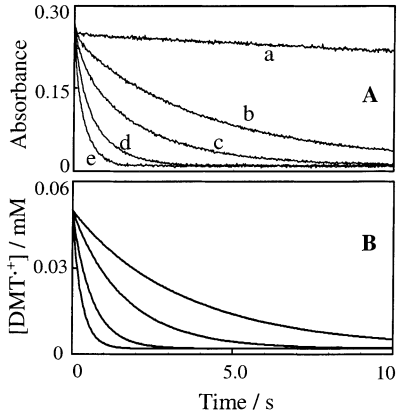

Figure 5. (A) Time changes in absorbance at 470 nm of DMT•+ observed after mixing the AN solution of 0.10 mM TBPA•+ with the AN solution of (a) 0.10, (b) 1.0, (c) 2.0, (d) 5.0, or (e)10.0 mM DMT. After mixing the concentration of DMT coexisting with 0.05 mM DMT•+ is (a) 0, (b) 0.45, (c) 0.95, (d) 2.45, (e) 4.95 mM, respectively. (B) Simulated results obtained assuming the rate law of $-d[DMT^{\bullet+}]/dt = k[DMT^{\bullet+}]\,[DMT]$ and using the identical k value of 6.5×10^2 M^{-1} s^{-1}.

of DMT•+, the decay curves of DMT•+ were recorded in the presence of several concentrations of DMT. Figure 5A shows the changes in absorbance at 470 nm, which is the absorption maximum of DMT•+ (Figure 4), depending on the concentration of DMT coexisted in the reaction solutions. As shown in Figure 5A, the decay rate of DMT•+ was accelerated with the increase of the concentration of DMT.

To analyze the effect of DMT quantitatively, simulation analysis was carried out for the decay curves b−e in Figure 5A. By taking into account the consumption of both DMT•+ and DMT during the reaction, and by using an identical value of k, 6.5×10^2 M^{-1} s^{-1}, numerical calculation was performed using computer software. Consequently, working curves showing the fairly good fit could be obtained as shown in Figure 5B by changing only the concentration of DMT on the basis of the rate law (eq 3).

$$-d[DMT^{\bullet+}]/dt = k[DMT^{\bullet+}]\,[DMT] \qquad (3)$$

This rate law means that the initial interaction between DMT•+ and DMT is the rate-determining step (rds). Considering the previous results of the electrochemical oxidation of DMT to form TMBT,[16,17] the proton extraction from DMT•+ by DMT can be regarded as the rds. That is, the acid−base interaction between DMT•+ and DMT is significant in the decay reaction of DMT•+ as in eq 4.

$$DMT^{\bullet+} + DMT \rightarrow (DMT\text{-}H)^{\bullet} + DMT(H^+) \qquad (4)$$

$$2\,(DMT\text{-}H)^{\bullet} \rightarrow TMBT \qquad (5)$$

If the acid−base reaction of eq 4 was in equilibrium, the protonated from of DMT (DMT(H+)), which increases with the progress of the reaction, should affect the decay rate of DMT•+ by participating in the rate law. Thus, the excellent fit with eq 3 in Figure 5B means that the acid−base reaction of DMT•+ and DMT is the rds. The redox reaction between DMT•+ and (DMT-H)• might be imaginable in the proposed scheme after eq 4. However, the consumption of one DMT•+ per one DMT was taken into account in the simulation of Figure 5B. Thus, after the rds, the dimerization reaction of two (DMT-H)• is considered to proceed rapidly.

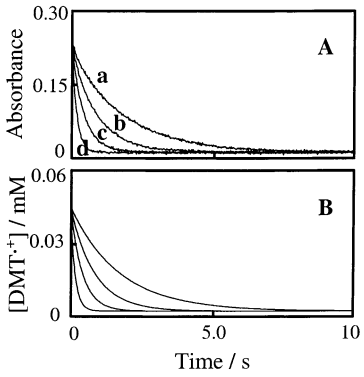

Figure 6. (A) Time changes in absorbance at 470 nm of DMT•$^+$ observed after mixing of the AN solution of 0.10 mM TBPA•$^+$ with the AN solution containing both 0.10 mM DMT and (a) 5.0, (b) 10.0, (c) 20.0, or (d) 50.0 mM Py. After the mixing, the concentration of Py coexisting with 0.05 mM DMT•$^+$ is (a) 2.5, (b) 5.0, (c) 10.0, and (d) 25.0 mM, respectively. (B) Simulated results obtained assuming the rate law of $-\mathrm{d}[\mathrm{DMT}\bullet^+]/\mathrm{d}t = k[\mathrm{DMT}\bullet^+]\,[\mathrm{Py}]$ and using the identical k value of $2.3 \times 10^2\ \mathrm{M}^{-1}\ \mathrm{s}^{-1}$.

In the above mechanism, by working as a base, DMT can promote the formation of TMBT. Such character of DMT as a base is reasonably expected because it is an amine compound. Thus, in the case of DMT, it was found that one electron brought about the conversion of the acidic and basic character between DMT•$^+$ and DMT (eq 6).

$$\underset{\text{(base)}}{\mathrm{DMT}} - \mathrm{e}^- \leftrightarrow \underset{\text{(acid)}}{\mathrm{DMT}\bullet^+} \qquad (6)$$

Effect of Pyridine Derivatives on the Reaction of DMT•$^+$. To clarify the Brønsted acid−base interaction to promote the decay reaction of DMT•$^+$, next we carried out the kinetic analysis of the reaction of DMT•$^+$ in the presence of X-Py s, because Py is known as a typical base in AN. In the ETSF method, this reaction is easily observable with no hindrances of DMT by mixing the AN solution of 0.10 mM TBPA•$^+$ with the AN solution containing both 0.10 mM DMT and varied concentration of X-Py. Because the oxidation potential of Py is much higher than that of TBPA,[21] the reaction between DMT•$^+$ and Py can be observed after the electron transfer of eq 2.

As a consequence, the acceleration of the decay reaction of DMT•$^+$ was observed with the increase of the concentration of Py as shown in Figure 6A, which was very similar to the result of Figure 5A. From the results of the simulation analysis, it was found that the rate law was expressed as eq 7, and k was determined to be $2.3 \times 10^2\ \mathrm{M}^{-1}\ \mathrm{s}^{-1}$.

$$-\mathrm{d}[\mathrm{DMT}\bullet^+]/\mathrm{d}t = k[\mathrm{DMT}\bullet^+]\,[\mathrm{Py}] \qquad (7)$$

Thus, the acid−base interaction to promote the decay reaction of DMT•$^+$ was verified using the typical base, Py, instead of DMT. The results of cyclic voltammetry also showed the qualitative promotion of the consecutive reactions as shown in Figure 7.

Substituent Effect of Pyridine Derivatives on the Decay Reaction Rates of DMT•$^+$. The effects of X-Py s on the reactions of DMT•$^+$ were systematically investigated using the ETSF method. Consequently, the rate law of eq 7 was obtained for all other seven derivatives examined, and the reaction rates, k, were determined to be: 2Me-Py, $5.0 \times 10^2\ \mathrm{M}^{-1}\ \mathrm{s}^{-1}$; 4Me-Py, $7.5 \times 10^2\ \mathrm{M}^{-1}\ \mathrm{s}^{-1}$; 2,4Me-Py, $1.55 \times 10^3\ \mathrm{M}^{-1}\ \mathrm{s}^{-1}$; 2,6Me-Py, $5.8 \times 10^2\ \mathrm{M}^{-1}\ \mathrm{s}^{-1}$; 2,4,6Me-Py, $1.7 \times 10^3\ \mathrm{M}^{-1}\ \mathrm{s}^{-1}$; 4CN−Py, $2.4 \times 10^{-1}\ \mathrm{M}^{-1}\ \mathrm{s}^{-1}$; 4MeO−Py, $1.45 \times 10^3\ \mathrm{M}^{-1}\ \mathrm{s}^{-1}$.

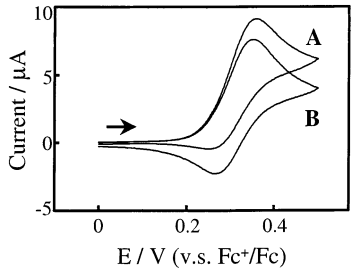

Figure 7. Cyclic voltammograms of 1.0 mM DMT in AN. (A) With 5.0 mM Py, (B) without Py. Supporting electrolyte: tetrabutylammonium hexafluorophosphate 0.10 M. Working electrode: platinum disk electrode (diameter: 1.6 mm). Scan rate: 100 mV s^{-1}.

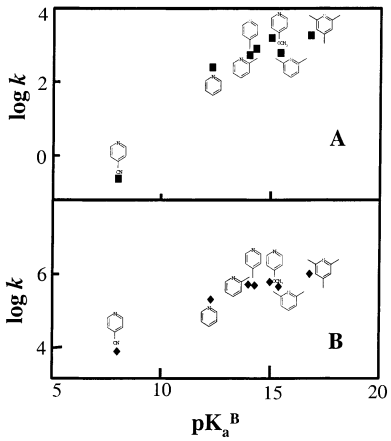

Figure 8. (A) Dependence of the reaction rates of DMT•$^+$ with X-Py s on the base strengths (pK_a^B, ref 18), together with (B) the previous result on the deprotonation rates of the hexamethylbenzene cation radical.[18]

The changes in the reaction rates involving pyridine derivatives have been investigated on the cation radical−nucleophile reaction[21] and the proton extraction reaction from the cation radicals.[18] The present results showed the relationship similar to the latter case,[18] in which the rates were plotted versus pK_a^B ($K_a^B = [\mathrm{X\text{-}Py}][\mathrm{H}^+]/[\mathrm{X\text{-}PyH}^+]$). Figure 8 shows the relationship between log k and pK_a^B in the present case, together with the previous result for the hexamethylbenzene cation radical.[18] This similarity supports a view that the decay reaction of DMT•$^+$ is promoted through the proton extraction by the coexisting Brønsted base molecules.

Reaction Products and Mechanisms. In the electrochemical method, it was established that the dimer compound, TMBT (Figure 1), was produced in the oxidation of DMT in AN.[16,17] In the present work, to investigate the products in the ETSF procedures, product analysis was carried out for the solution after mixing TBPA•$^+$ and DMT. As a result, the formation of TMBT as a main product is also confirmed. Thus, the reaction mechanisms can be summarized as shown in Figure 9. After the rate determining proton extraction by DMT, the coupling reaction of two radical species, (DMT-H)•, proceeds to form TMBT.

The product analysis was also performed for the products obtained in the reactions with X-Py s. In the presence of Py, the result of NMR showed the isolated main product was *N*, *N*′-dimethyl-*N*, *N*′-di-*p*-tolylethylenediamine (DMDTE). That is, the proton extraction was found to occur at the *N*-methyl position. As well as the remarkable difference in the NMR

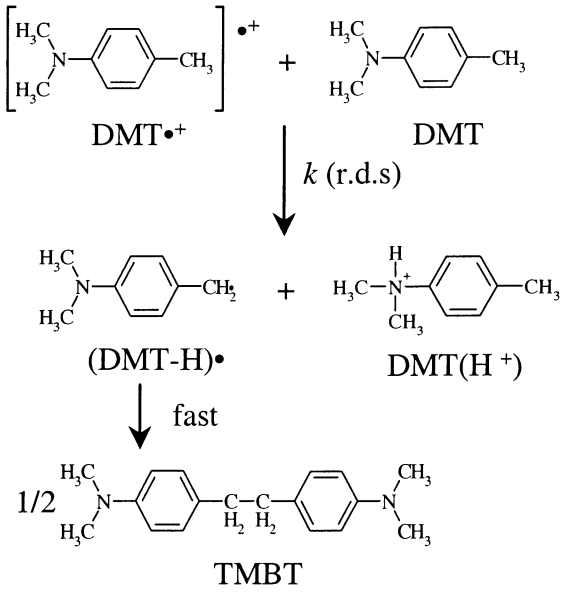

Figure 9. Mechanism of the dimerization reaction of DMT•+ with the presence of DMT.

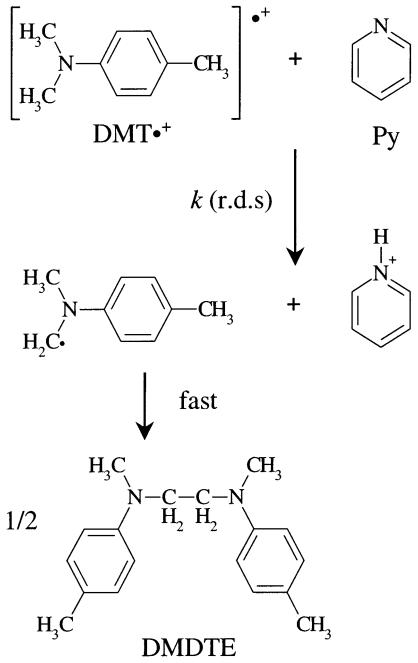

Figure 10. Mechanism of the dimerization reaction of DMT•+ with the presence of Py.

results, TMBT and DMDTE can be distinguished in a thin-layer chromatography. Thus, the products in the reactions with the other seven X-Py s were examined using the thin-layer chromatography. Consequently, the main product in the presence of X-Py s was identified to be DMDTE in all the cases. Thus, the reaction mechanism with Py can be summarized as Figure 10, and this is true for the other X-Py s.

Except the final product, both the reaction schemes are essentially the same; after the rate determining proton extraction by DMT or Py, the coupling reaction of two radical species proceeds. The present results of the products analysis showed that a proton of *N*-methyl group of DMT•+ is subtracted by Py, while a proton of *p*-methyl group is subtracted by the neutral DMT. The reason for this difference is unclear at present. However, the formation of DMDTE was reported in the reaction of DMT and *tert*-butoxy radical through a proton extraction from

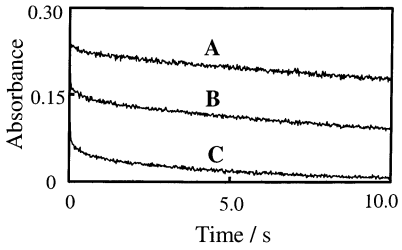

Figure 11. Time changes in absorbance at 470 nm of DMT•+ observed after mixing of the AN solution of 0.10 mM TBPA•+ with the AN solution containing both 0.10 mM DMT and (A) 2.5, (B) 5.0, or (C) 7.5 M DMF. After mixing, the concentration of DMF coexisting with 0.05 mM DMT•+ is (a) 1.25, (b) 2.50, and (c) 3.75 M, respectively.

the *N*-methyl group.[22] Thus, the formation of DMDTE does not seem to be exceptional. Rather than DMDTE, it might be better to consider a specific interaction for the formation of TMBT, e.g., the π-π stacking interaction between DMT•+ and DMT to promote the H^+ extraction from the *p*-methyl group of DMT•+. However, this is a merely possible speculation from the reaction products.

Decay Reaction of DMT•+ in the Presence of DMF. Amatore and co-workers revealed the reaction mechanisms of aromatic amine derivative cation radicals using the fast scan cyclic voltammetry, in which DMF was used as a solvent.[8,9] While the basic property of the neutral substrate was considered in the case of *p*-anisidine,[8] the interaction with DMF as a base was significant in the cases of *p*-halogenoanilines.[9]

To evaluate the basic property of the present case of DMT, we observed the decay reaction of DMT•+ in the presence of DMF in the AN solutions. Figure 11 shows the decay curves of DMT•+ observed after mixing the solution of DMT•+ in AN with the solution containing 2.5, 5.0, or 7.5 M DMF in AN. Compared with the absorbance change of only DMT•+ in AN (Figure 5Aa), remarkable decrease was found in the cases with a large excess of DMF, though the change in Figure 11 is quite different from Figures 5A and 6A (i.e., do not follow a certain rate law). However, if the solvent was totally replaced to DMF, it is expected that DMT•+ diminished totally even just after the mixing in the optical cell. Thus, the basic property of DMF (if it is used as the solvent) is considered to be stronger than that of the neutral DMT (used as the reactant).

The present ETSF method can be utilized for such comparison and the evaluation of basic properties. In the present work, despite the relative lower basic property of DMT compared with *p*-anisidine,[8] which is suspected via DMF solvent, the significant contribution of the neutral DMT to the decay reaction of DMT•+ was clearly revealed in AN.

Conclusions

In the present work, first, the stability of DMT•+ in the absence of DMT in AN has been revealed using the ETSF method, though the previous electrochemical work reported the instability of DMT•+; e.g., the spectroscopic detection of DMT•+ in AN had been very difficult.[16] This can be attributed to the difference between the ETSF and electrochemical methods. In the electrochemical oxidation, the neutral DMT molecules surely exist in bulk solution, so that the reaction of DMT•+ is promoted by the basic property of DMT. The function of DMT as a base is a significant driving force of the CH_2−CH_2 bond formation in the reaction of DMT•+.

For the electrochemical dimerization reactions of aromatic cation radicals, mechanistic attention has been devoted to the terms of "the radical−radical coupling" (RRC) or "the radical−

substrate coupling" (RSC) mechanisms.[20] In the present case, the RRC is very slow, if at all, as revealed in the absence of the substrate DMT (Figure 5Aa). This is quite reasonable considering the blocking effect of *p*-methyl group, while the RRC mechanism was confirmed for methyldiphenylamine and diphenylamine cation radicals.[11,12] Whereas the RSC implies the direct coupling reaction in many cases,[20,23] the present reaction can be regarded as an interesting example. This is because little kinetic attention has been paid on the acid−base interaction of the present type, despite the rate law being identical to the RSC (when the first encounter step is the rds).

In the elucidation of the reactions of cation radicals, in some cases, it might be necessary to take into account that such acid−base interactions with the neutral molecules surely exist in solution. While the voltammetric measurements were usually carried out at a certain concentration, ca. 1 mM or so, diverse changes in the concentration of the neutral molecules versus the cation radicals, as in the present work, would be necessary to clarify the such interaction.

Indeed, DMT would be a special case because a proton of the *p*-methyl group is key as the acidic property, while N is the source of the basic property. However, it is of interest that such Brønsted acid−base character can be converted by one electron.

While complex aspects of the electrochemical oxidation of DMT were reported previously,[16,17] in the present ETSF analysis, neither the formation of the oxidation product of TMBT nor the distortion of the decay curve by the protonated form of TMBT was observed. Thus, the ETSF method has permitted the straightforward analysis and given a definite kinetic conclusion concerning the RS acid−base reaction between $DMT^{\bullet+}$ and DMT. Although the changes in cyclic voltammograms of DMT in Figures 3 and 7 should be reasonable when we consider that the contribution of the bases, it would be difficult to define the mechanism on the basis of only the voltammograms. Thus, in the mechanistic elucidation of the electrochemical oxidation processes involving aromatic cation radicals, the ETSF method would be effective as a complementary tool.

Acknowledgment. This work was supported in part by a Grant-in-Aid for Scientific Research from the Ministry of Education, Culture, Science, Sports and Technology, Japan, No. 13640602. M.O. thanks the Mitsubishi Foundation for the financial support. H.P. thanks the JSPS (Japan Society for the Promotion of Science) Postdoctoral Fellowship for Foreign Researchers.

References and Notes

(1) Parker, V. D. *Acc. Chem. Res.* **1984**, *17*, 243.
(2) Parker, V. D.; Chao, Y.; Reitstöen, B. *J. Am. Chem. Soc.* **1991**, *113*, 2336.
(3) Parker, V. D.; Chao, Y. T.; Zheng, G. *J. Am. Chem. Soc.* **1997**, *119*, 11390.
(4) Parker, V. D.; Zhao, Y.; Lu, Y.; Zheng, G. *J. Am. Chem. Soc.* **1998**, *120*, 12720.
(5) Lu, Y.; Zhao, Y.; Parker, V. D. *J. Am. Chem. Soc.* **2001**, *123*, 5900.
(6) Tschuncky, P.; Heinze, J.; Smie, A.; Engelmann, G.; Kossmehl, G. *J. Electroanal. Chem.* **1997**, *433*, 223.
(7) Heinze, J.; John, H.; Dietrich, M.; Tschunky, P. *Synth. Met.* **2001**, *119*, 49.
(8) Simon, P.; Farsang, G.; Amatore, C. *J. Electroanal. Chem.* **1997**, *435*, 165.
(9) Amatore, C.; Farsang, G.; Maisonhaute, E.; Simon, P. *J. Electroanal. Chem.* **1999**, *462*, 55.
(10) Oyama, M.; Goto, M.; Park, H. *Electrochem. Commun.* **2002**, *4*, 110.
(11) Oyama, M.; Higuchi, T.; Okazaki, S. *Electrochem. Commun.* **2000**, *2*, 675.
(12) Oyama, M.; Higuchi, T.; Okazaki, S. *J. Chem. Soc., Perkin Trans. 2* **2001**, 1287.
(13) Oyama, M.; Higuchi, T.; Okazaki, S. *Electrochem. Commun.* **2001**, *3*, 363.
(14) Oyama, M.; Higuchi, T. *J. Electrochem. Soc.* **2002**, *149*, E12.
(15) Oyama, M.; Higuchi, T.; Okazaki, S. *Electrochem. Solid-State Lett.* **2002**, *5*, E1.
(16) Melicharek, M.; Nelson, R. F. *J. Electroanal. Chem.* **1970**, *26*, 201.
(17) Hand, R.; Melicharek, M.; Scoggin, D. I.; Stotz, R.; Carpenter, A. K.; Nelson, R. F. *Coll. Czech. Chem. Commun.* **1971**, *36*, 842.
(18) Schlesener, C. J.; Amatore, C.; Kochi, J. K. *J. Am. Chem. Soc.* **1984**, *106*, 7472.
(19) Eberson, L., Larsson, B. *Acta Chim. Scand. B* **1986**, *40*, 210.
(20) Schmittel, M.; Burghart, A. *Angew. Chem., Int. Ed. Engl.* **1997**, *36*, 2550.
(21) Reitstöen, B.; Parker, V. D. *J. Am. Chem. Soc.* **1991**, *113*, 6954.
(22) Henbest, H. B.; Patton, R. *Proc. Chem. Soc.* **1959**, 225.
(23) Nozaki, K.; Oyama, M.; Okazaki, S. *J. Electroanal. Chem.* **1989**, *270*, 191.